

---

# Collars and Intestines: Practical Conforming Delaunay Refinement

Alexander Rand and Noel Walkington

Carnegie Mellon University

**Summary.** While several existing Delaunay refinement algorithms allow acute 3D piecewise linear complexes as input, algorithms producing conforming Delaunay tetrahedralizations (as opposed to constrained or weighted Delaunay tetrahedralizations) often involve cumbersome constructions and are rarely implemented. We describe a practical construction for both “collar” and “intestine”-based approaches to this problem. Some of the key ideas are illustrated by the inclusion of the analogous 2D Delaunay refinement algorithms, each of which differs slightly from the standard approach. We have implemented the 3D algorithms and provide some practical examples.

## 1 Introduction

Acute input angles pose significant challenges to Delaunay refinement algorithms for quality mesh generation in both two and three dimensions. In 2D, the formation of a conforming mesh is relatively simple: acutely adjacent input segments must be split at equal lengths. Research extending Ruppert’s algorithm [16] to accept small input angles [17, 8] focused on finding algorithms which involve simple modifications of Ruppert’s algorithm and produce the “best” output meshes in practice. In 3D, producing a conforming tetrahedralization of an arbitrary piecewise linear complex (PLC) involves a substantial construction [10, 6] and quality refinement algorithms have been developed in the context of this construction [5, 11]. Alternative algorithms involving weighted [4, 3] and constrained [17, 19, 18] Delaunay tetrahedralization have also been developed. Due to these different challenges, the algorithms for 3D Delaunay refinement of acute domains are markedly different than those in 2D.

In this paper, we describe two related strategies for the protection of acute angles during 3D Delaunay refinement: collars and intestines. The collar approach generalizes the construction of Murphy, Mount, and Gable [10] and that of Cohen-Steiner, Colin de Verdière, and Yvinec [6] and produces a

quality mesh following the ideas of Pav and Walkington [11]. The intestine approach is closely related to the quality refinement algorithm of Cheng and Poon [5]. Unlike these previous algorithms for 3D Delaunay refinement of acute input, our algorithms are motivated by analogous 2D versions and, more notably, have been implemented.

---

**Algorithm 1** Quality Refinement of Acute Input

---

(PROTECT) Protect acute input angles.

(REFINE) Perform a protected version of Ruppert’s algorithm.

---

Algorithm 1 is the template for both the collar and intestine based refinement algorithms. The (PROTECT) step requires information about the  $(d - 2)$ -dimensional features of the input complex. We note that a brute force computation of this information can be avoided using estimates resulting from certain Delaunay refinement algorithms [13, 14] or an exact computation during sparse Voronoi refinement [9].

Section 2 contains necessary preliminaries for our analysis. Section 3 describes both collar and intestine based Delaunay refinement algorithms in two dimensions, and the three-dimensional algorithms are given in Section 4. Finally, some examples and practical issues are discussed in Section 5.

## 2 Preliminaries

### 2.1 Definitions

Our algorithms accept an arbitrary PLC as input and involve an intermediate piecewise smooth complex (PSC), defined below.

**Definition 1.** *In three dimensions [or two dimensions]:*

- A **piecewise linear complex** (PLC),  $C = (\mathcal{P}, \mathcal{S}, \mathcal{F})$  [ $(\mathcal{P}, \mathcal{S})$ ], is a triple [duple] of sets of input vertices  $\mathcal{P}$ , input segments  $\mathcal{S}$ , and polygonal input faces  $\mathcal{F}$  such that the boundary of any feature or the intersection of any two features is the union of lower-dimensional features in the complex.
- A PLC  $C' = (\mathcal{P}', \mathcal{S}', \mathcal{F}')$  [ $(\mathcal{P}', \mathcal{S}')$ ] is a **refinement** of the PLC  $C = (\mathcal{P}, \mathcal{S}, \mathcal{F})$  if  $\mathcal{P} \subset \mathcal{P}'$ , each segment in  $\mathcal{S}$  is the union of segments in  $\mathcal{S}'$ , and every face in  $\mathcal{F}$  is the union of faces in  $\mathcal{F}'$ .
- A **piecewise smooth complex** (PSC),  $C = (\mathcal{P}, \mathcal{S}, \mathcal{F})$  [ $C = (\mathcal{P}, \mathcal{S})$ ], is a triple [duple] of sets of input vertices  $\mathcal{P}$ , non-self-intersecting smooth input curves  $\mathcal{S}$ , and non-self-intersecting smooth input faces  $\mathcal{F}$  such that the boundary of any feature or the intersection of any two features is the union of lower-dimensional features in the complex.

**Definition 2.** Let  $C$  be a PLC.

- The  **$i$ -local feature size** at point  $x$  with respect to  $C$ ,  $\text{lfs}_i(x, C)$ , is the radius of the smallest closed ball centered at  $x$  which intersects two disjoint features of  $C$  of dimension no greater than  $i$ .
- The **1-feature size** of segment  $s$  with respect to  $C$ ,  $\text{fs}_1(s, C)$ , is the radius of the smallest closed ball centered at a point  $x \in s$  intersecting a segment or input vertex of  $C$  which does not intersect  $s$ .

If the argument supplied to the local feature size function is a set of points, rather than a single point, then the result is defined to be the infimum of the function over the set, i.e.  $\text{lfs}_i(s, C) := \inf_{x \in s} \text{lfs}_i(x, C)$ . Often the PLC argument supplied to the local feature size is that of the input complex and in this case the argument will be omitted. The subscript will be omitted when it is equal to  $(d - 1)$  where  $d$  is the dimension, i.e.  $\text{lfs}(x) := \text{lfs}_2(x)$  in 3D.

For a PSC we will use the same definition of local feature size as for a PLC. Typically the definition of local feature size for a PSC also involves the radius of curvature or the distance to the medial axis. Since we will only use a very restricted class of PSCs the simpler definition is sufficient. In our particular constructions the radius of curvature is proportional to (and often equal to) the local feature size defined above.

## 2.2 Generic Delaunay Refinement Algorithm

---

### Algorithm 2 Delaunay Refinement

---

```

Create an initial Delaunay triangulation.
Queue all unacceptable simplices.
while the queue of simplices is nonempty do
    if it is safe to split the front simplex then
        Take an action based on the front simplex.
        Queue additional unacceptable simplices.
    end if
    Remove the front simplex from the queue.
    Dequeue any queued simplices which no longer exist.
end while
    
```

---

The Delaunay refinement algorithms which we will consider have the form of Algorithm 2. Additionally, we require that each of the operations involve only local computations in the Delaunay triangulation of the current vertex set. To specify an algorithm from Algorithm 2, it is necessary to carefully describe the following four statements.

Action	Where should a vertex be inserted to “split” a simplex? Should other simplices be added to the queue?
Priority	In what order should the queue be processed?
Unacceptability	Which simplices are unacceptable?
Safety	Which simplices are safe to split?

### 3 Delaunay Refinement in 2D

Before describing the full 3D algorithms, analogous 2D Delaunay refinement algorithms are given. The resulting algorithms are similar to those typically used for Delaunay refinement in the presence of acute input angles [17, 8], but avoid certain challenges which are difficult to extend to 3D.

We will describe the two steps in the refinement of an arbitrary PLC given in Algorithm 1: acute input angles are first protected, and then Delaunay refinement is performed. We assume that an appropriate estimate of the local feature size is available at each input vertex. Specifically, we require that for each  $q_0$  which is the vertex of an acute input angle, we are given a distance  $d_{q_0}$  which satisfies  $b \cdot \text{lfs}(q_0) \leq d_{q_0} \leq \min(c_0 \cdot \text{lfs}_0(q_0), c_1 \cdot \text{lfs}(q_0))$  for some constants  $b > 0$ ,  $c_0 \in (0, .5)$  and  $c_1 \in (0, 1)$ .

#### 3.1 Collar Protection Region

A collar protection region involves forming “collar” segments of equal length around each input vertex so that the Delaunay triangulation conforms to the input near this vertex. The subsequent Delaunay refinement algorithm will then prevent the insertion of any vertices which encroach this collar region.

##### (PROTECT) Formation of the Protection Region

For each  $q_0$  which is the vertex of an acute input angle, each input segment containing  $q_0$  is split at a distance  $d_{q_0}$  away from  $q_0$ . Figure 3.1 depicts an example of the points inserted during this step.

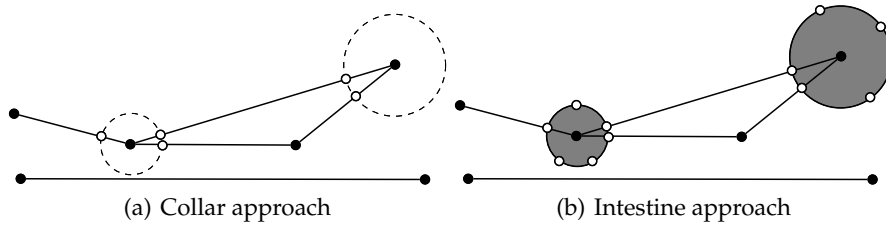


Fig. 1. Two different protection approaches.

Each end segment containing the vertex of an acute input angle will be called a collar simplex and vertices inserted during this step are called collar vertices. First, we observe that the collar simplices are sufficiently far away from disjoint input features of  $C$ .

**Lemma 1.** *For any input point  $q_0 \in \mathcal{P}$ ,*

$$\begin{aligned} \text{dist}(B(q_0, d_{q_0}), B(q'_0, d_{q'_0})) &\geq (1 - 2c_0) \text{lfs}(q_0) \text{ for all } \mathcal{P} \ni q'_0 \neq q_0 \text{ and} \\ \text{dist}(B(q_0, d_{q_0}), s) &\geq (1 - c_1) \text{lfs}(q_0) \text{ for all segments } s \not\ni q_0. \end{aligned}$$

Let  $\alpha$  be the smallest angle between adjacent segments in  $C$  and let  $\bar{C}$  denote the refined PLC obtained after inserting all of the collar vertices. The next lemma quantifies the relationship between the local feature size of  $\bar{C}$  and  $C$ .

**Lemma 2.** *There exists  $K > 0$  depending only on  $b$  and  $c_0$  such that for all  $x$ ,*

$$\text{lfs}(x, \bar{C}) \leq \text{lfs}(x, C) \leq \frac{K}{\sin(\alpha)} \text{lfs}(x, \bar{C}).$$

With the protection region in place, Delaunay refinement can now be performed.

## (REFINE) Protected Delaunay Refinement

This step is the Delaunay refinement algorithm described in Algorithm 3 (by specializing Algorithm 2). Each new end segment is “protected” during refinement: no vertices will be inserted in the diametral ball of these segments. To ensure this, circumcenters which encroach these end segments are rejected by the safety criteria. Lemma 1 ensures that no inserted midpoints encroach upon a collar simplex and thus the diametral disk of each collar simplex will be empty throughout the algorithm.

---

**Algorithm 3** 2D Delaunay Refinement With Collar
 

---

Action	Insert the circumcenter of a simplex unless it causes a lower-dimensional simplex to be unacceptable. In this case, queue the lower-dimensional simplex.
Priority	Segments are given higher priority than triangles.
Unacceptability	A segment with a non-empty diametral disk is unacceptable. A triangle with radius-edge ratio larger than $\tau$ is unacceptable.
Safety	Collar simplices are not safe to split.

---

The termination of the algorithm and properties of the resulting mesh are described in Theorems 1 and 2. The first theorem ensures that the algorithm

terminates and the resulting mesh is graded to the local feature size, and the second theorem asserts that the mesh conforms to the input PLC and specifies which triangles near collar simplices may have poor quality.

**Theorem 1.** *For any  $\tau > \sqrt{2}$ , there exists  $K > 0$  depending only upon  $\tau$ ,  $b$ , and  $c_0$  such that for each vertex  $q$  inserted by Algorithm 3,*

$$\text{lfs}(q, C) \leq \frac{K}{\sin(\alpha)} r_q.$$

*Remark 1.* The inequality  $\text{lfs}(q, \tilde{C}) \leq K r_q$  is shown using an argument identical to the standard analysis of Ruppert's algorithm. Then Lemma 2 yields the desired inequality.

**Theorem 2.** *Algorithm 3 produces a conforming Delaunay triangulation of  $C$ . The circumcenter of any remaining triangle with radius-edge ratio larger than  $\tau$  lies in the diametral disk of a collar simplex.*

### 3.2 Intestine Protection Region

The intestine protection region yields the added result that no triangles in the resulting mesh have angles larger than  $\pi - 2\kappa$ , where  $\kappa := \sin^{-1}\left(\frac{1}{2\tau}\right)$  is the minimum angle corresponding to the radius-edge threshold  $\tau$ .

#### (PROTECT) Formation of the Protection Region

For each input vertex  $q_0$  at an acute input angle, all input segments containing  $q_0$  are split at a distance  $d_{q_0}$  away from  $q_0$ . Additionally, vertices are added such that all arcs of the circle centered at  $q_0$  with radius  $d_{q_0}$  are no larger than  $\frac{\pi}{2}$ . This ensures that the diametral ball of each arc of the circle does not contain  $q_0$  and requires at most three additional vertices per input vertex.

We will now consider a PSC  $\hat{C}$  defined by the input PLC, vertices inserted on each segment at distance  $d_{q_0}$  from each input vertex  $q_0$  (as in the collar protection region), and the boundary arcs of each disk  $B(q, d_q)$  as depicted in Figure 3.1. The essential property of the PSC  $\hat{C}$  is that all acute angles between features occur between segments of  $C$  and are contained in  $\bigcup_{q_0} B(q_0, d_{q_0})$ . Let  $\alpha$  again denote the smallest angle between adjacent segments of  $C$ . The local feature sizes with respect to  $C$  and  $\hat{C}$  are related, as described in the next lemma.

**Lemma 3.** *There exists  $K > 0$  depending only on  $b$ ,  $c_0$ , and  $c_1$  such that for all  $x$ ,*

$$\text{lfs}(x, \hat{C}) \leq \text{lfs}(x, C) \leq \frac{K}{\sin(\alpha)} \text{lfs}(x, \hat{C}).$$

A suitably sized protection region has been formed and now the subsequent Delaunay refinement algorithm can be described and analyzed.

(REFINE) Protected Delaunay Refinement

Ruppert's algorithm can be performed *outside* of  $\bigcup_{q_0} B(q_0, d_{q_0})$  and each of the boundary arcs of any disk  $B(q_0, d_{q_0})$  is protected by the diametral disk of its endpoints. This is described completely in Algorithm 4. Refinement of general PSCs in 2D by algorithms similar to Ruppert's has been considered [1, 2, 12] and our analysis follows these developments.

---

**Algorithm 4** 2D Delaunay Refinement With Intestine
 

---

Action	Insert the circumcenter of a simplex unless it causes a lower-dimensional simplex or arc to be unacceptable. In this case, queue the lower-dimensional object. Insert the midpoint of an arc.
Priority	Segments and arcs are given higher priority than triangles.
Unacceptability	A segment or arc with a non-empty diametral disk is unacceptable. A triangle with radius-edge ratio less than $\tau$ is unacceptable.
Safety	All simplices and arcs are safe to split.

---

Algorithm 4 terminates and produces a conforming graded mesh as described in the following two theorems.

**Theorem 3.** *For any  $\tau > \sqrt{2}$ , there exists  $K > 0$  depending only upon  $\tau$ ,  $b$ ,  $c_0$ , and  $c_1$  such that for each vertex  $q$  inserted by Algorithm 4,*

$$\text{lfs}(q, C) \leq \frac{K}{\sin(\alpha)} r_q.$$

*Remark 2.* Unlike Theorem 1, the proof of Theorem 3 is substantially more involved than the usual proof for Ruppert's algorithm. This is a result of the smooth input features of  $\hat{C}$ . Using the techniques of Theorem 1, Theorem 3 can be shown with the strong restriction that  $\tau > 2$ .

**Theorem 4.** *Algorithm 4 produces a conforming Delaunay triangulation of  $C$ . Any remaining triangle with radius-edge ratio larger than  $\tau$  is inside  $B(q_0, d_{q_0})$  for some input vertex  $q_0$ . The resulting triangulation contains no angles larger than  $\pi - 2\kappa$ .*

## 4 Delaunay Refinement in 3D

Producing a conforming Delaunay tetrahedralization of a 3D PLC requires a consistent mesh along segments between acutely adjacent features. To initially form this consistent mesh we require the feature size to be known along segments of the input mesh. Given a PLC  $C = (\mathcal{P}, \mathcal{S}, \mathcal{F})$ , we will assume that we have a refinement  $C_1 = (\mathcal{P}_1, \mathcal{S}_1, \mathcal{F})$  such that

- (H1)  $(\mathcal{P}' \setminus \mathcal{P}) \setminus (\cup_{s \in \mathcal{S}} s) = \emptyset$ ,  
(H2) for any  $q_0 \in \mathcal{P}$ , all  $s_1 \in \mathcal{S}_1$  such that  $q_0 \in s_1$  have equal length satisfying  $|s_1| \leq c_0 \cdot \text{lfs}_0(q_0)$ , and  
(H3) for all  $s_1 \in \mathcal{S}_1$ ,  $b \cdot \min(\text{fs}_1(s_1), \text{lfs}(s_1)) < |s_1| < c_1 \cdot \min(\text{fs}_1(s_1), \text{lfs}(s_1))$ ,  
where  $b > 0$ ,  $c_0 \in (0, .5)$ , and  $c_1 \in (0, 1)$  are some constants.

#### 4.1 Collar Protection Region

(PROTECT) Formation of the Protection Region

For each input face, the collar is formed by inserting vertices according to the following rules.

1. If  $s$  and  $s'$  are adjacent non-end segments which meet at vertex  $q$ , then a vertex  $p$  is inserted at distance  $\frac{\max(|s|, |s'|)}{2}$  from  $q$ , in any direction into the face perpendicular to  $s$ .
2. If  $s$  is an end segment and  $s'$  is an adjacent non-end segment, both containing vertex  $q$ , then insert vertex  $p$  at the intersection of any line parallel to  $s$  in the face at distance  $\frac{|s'|}{2}$  away from  $s$  and on the circle of radius  $|s|$  around the input point on  $s$ .
3. For any input vertex  $q_0$  on a segment  $s$ , insert collar vertices such that the sphere of radius  $|s|$  around  $q_0$  restricted to the face has no arcs of angle larger than  $\frac{\pi}{2}$ .

Below is a list of objects defined to describe the collar based on the vertices inserted during this step. These objects are depicted in Figure 2(a).

<b>Collar Vertex</b>	A vertex inserted during the (PROTECT) step or as a mid-point of a collar segment or arc during the (REFINE) step.
<b>Collar Segment</b>	A segment between collar vertices corresponding to adjacent vertices on an input segment.
<b>Collar Arc</b>	An arc between adjacent collar vertices corresponding to the same input vertex.
<b>Collar Region</b>	The region between input segments and collar segments and arcs.
<b>Collar Simplex</b>	A simplex in the Delaunay triangulation of the face which lies inside the collar region.

Following the insertion of the collar vertices, the resulting Delaunay tetrahedralization satisfies a number of properties given in the following lemma.



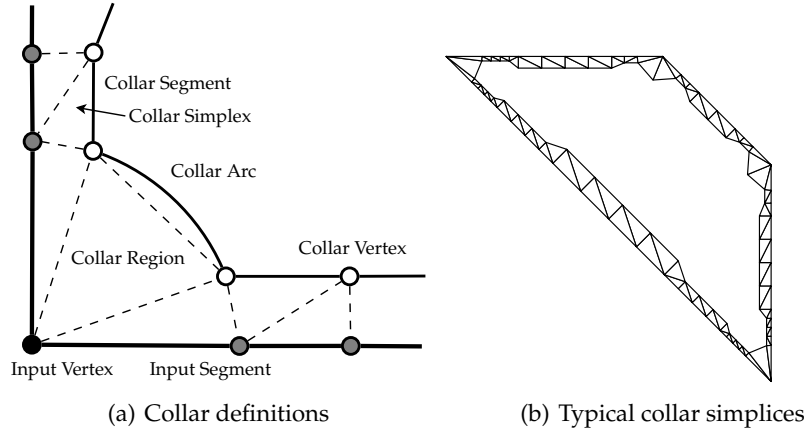


Fig. 2. Collar region

**Lemma 4.** *After inserting collar vertices, the following properties hold.*

- (I) *All adjacent collar segments and arcs meet at non-acute angles.*
- (II) *The diametral disk of each collar segment contains no vertices in  $\mathcal{P}'$ .*
- (III) *The circumball of any collar simplex contains no vertices in  $\mathcal{P}'$ .*
- (IV) *The circumball of any collar simplex does not intersect any disjoint faces or segments.*

*Remark 3.* The circumball of a simplex refers to the *smallest* open sphere such that all vertices of the simplex lie on the boundary of the sphere.

Since the circumball of each collar simplex is empty, the collar simplices conform to the input. Collar segments meet non-acutely and thus the complement of the collar region in each face is well-suited for Ruppert's algorithm. The final property is needed to guarantee that subsequent vertices inserted for conformity will not encroach upon disjoint collar simplices.

The collar divides each face into two regions: the collar region and the non-collar region. Let  $\bar{C}$  be the PSC including each face divided into its collar and non-collar regions and all collar segments and arcs. Let  $\alpha_1$  be the smallest angle between an input segment and another adjacent input feature in the mesh and let  $\alpha_2$  be the smallest angle between adjacent input faces. The next lemma asserts that this augmented complex  $\bar{C}$  preserves the initial local feature size, up to a factor depending on  $\alpha_1$  and  $\alpha_2$ .

**Lemma 5.** *There exists a constant  $K > 0$  depending only upon  $b$ ,  $c_0$ , and  $c_1$  such that*

$$\text{lfs}(x, \bar{C}) \leq \text{lfs}(x, C) \leq \frac{K}{\sin \alpha_1 \sin \alpha_2} \text{lfs}(x, \bar{C}).$$

As usual, the protection procedure is followed by a Delaunay refinement algorithm.

(REFINE) Protected Delaunay Refinement

The PSC  $\tilde{C}$  is now refined based on both quality and conformity criteria using a modified version of Ruppert’s algorithm. Similarly to the non-acute case, any maximum radius-edge threshold  $\tau > 2$  can be selected for determining poor quality tetrahedra. The Delaunay refinement algorithm is specified in Algorithm 5.

**Algorithm 5** 3D Delaunay Refinement With Collar

Action	Insert the circumcenter of a simplex unless it causes a lower-dimensional simplex, collar segment, or collar arc to be unacceptable. In this case, queue the lower-dimensional object. Insert the midpoint of a collar arc.
Priority	Collar segments and arcs are given the highest priority. Other simplices are prioritized by dimension with lower-dimensional simplices processed first.
Unacceptability	A simplex, collar segment, or collar arc is unacceptable if it has a nonempty circumball. A tetrahedron is unacceptable if its radius-edge ratio is larger than $\tau$ .
Safety	It is not safe to split any collar simplex (this includes both triangles in input faces and subsegments of input segments).

The key difference between Algorithm 5 and the 3D version of Ruppert’s algorithm is the safety criteria. This prevents the cascading encroachment associated with acutely adjacent segments and faces. Since collar arcs must be protected, analysis of the 3D refinement with the *collar* protection scheme is closely related to the 2D refinement with the *intestine* protection scheme.

During the algorithm, it is important to ensure that the properties of the collar in Lemma 4 continue to hold while allowing refinement of the non-collar region of each face to create a conforming mesh. In the 2D collar protection procedure, the collar simplices (i.e. the end segments) never change during Algorithm 3. In 3D however, the set of collar simplices does change. This occurs when the standard Delaunay refinement algorithm seeks to insert a vertex in a face that encroaches upon a collar segment or collar arc. Instead of adding this encroaching vertex, this collar segment or arc is split. This new vertex is a collar vertex and the collar segment or arc is replaced with two new collar segments or arcs. The collar *region* has not changed but the set of collar *simplices* has changed. Further, this new vertex may encroach upon the circumball of another collar simplex in an adjacent face. In this face, the collar segment associated with this encroached circumball is also split so that the

collar simplices on adjacent faces again “line up.” So conformity of the mesh is maintained by only splitting the collar segments and thus the algorithm never attempts to insert the circumcenter of an encroached collar simplex.

Several key properties hold throughout the algorithm whenever there are no collar segments or collar arcs on the queue.

**Lemma 6.** *If the queue of unacceptable simplices does not contain any collar segments or collar arcs, the following properties hold.*

- (I) *Adjacent collar segments and arcs meet at non-acute angles.*
- (II) *The circumball of any collar element contains no vertices in  $\mathcal{P}'$ .*

The first property is important to guarantee the termination of the algorithm, while the second property is important for ensuring the resulting tetrahedralization conforms to the input. These two facts are stated precisely in the next two theorems. Recall that  $\alpha_1$  is the smallest angle between an input segment and an adjacent feature while  $\alpha_2$  is the smallest angle between adjacent input faces.

**Theorem 5.** *For any  $\tau > 2$ , there exists  $K > 0$  depending only upon  $\tau$ ,  $b$ ,  $c_0$ , and  $c_1$  such that for each vertex  $q$  inserted by Algorithm 5,*

$$\text{lfs}(q, C) \leq \frac{K}{\sin \alpha_1 \sin \alpha_2} r_q.$$

*Remark 4.* Since  $\bar{C}$  includes smooth arcs, the proof of Theorem 5 involves many of the techniques used in Theorem 3.

**Theorem 6.** *Algorithm 5 produces a conforming Delaunay tetrahedralization of  $C$ . The circumcenter of any remaining tetrahedra with radius-edge ratio larger than  $\tau$  lies in the circumball of a collar simplex.*

## 4.2 Intestine Protection Region

The intestine approach for protecting acute input angles mirrors that in 2D described in Section 3.2. Smooth features will be added to the input to isolate all input segments and vertices (or at least those contained in acutely adjacent features) from the region to be refined for tetrahedron quality.

### (PROTECT) Formation of the Protection Region

The vertices and features which are added to the mesh in this step are a superset of those added during the (PROTECT) step of the collar approach (which created the PSC  $\bar{C}$ ). In addition to features of  $\bar{C}$ , the following objects are included to form a new PSC  $\hat{C}$ .

- For each input vertex  $q_0$  which belongs to some segment let  $d_{q_0}$  be the length of all segments containing  $q_0$ . Then  $\hat{C}$  includes  $\partial B(q_0, d_{q_0})$ .

- For each collar segment  $s$  let  $c$  be the surface of revolution produced by revolving segment  $s$  about its associated input segment. The features  $c$  and  $\partial c$  are included in  $\hat{C}$ .

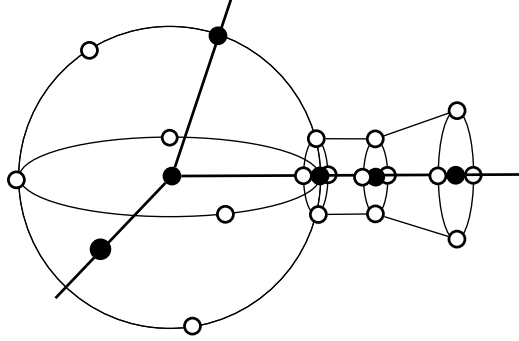


Fig. 3. Intestine Protection Region

The region inside each sphere and cylindrical surface added to the mesh will be called the intestine region and the remaining volume is called the non-intestine region. This is depicted in Figure 3. This construction is designed to ensure the following fact.

**Lemma 7.** *The non-intestine region of the PSC  $\hat{C}$  contains no acute angles between features.*

This lemma is necessary to ensure that the usual proof of termination and grading will apply to Delaunay refinement in the non-intestine region. Let  $\alpha_1$  and  $\alpha_2$  denote the smallest angles in the input as discussed previously.

**Lemma 8.** *There exists  $K > 0$  depending only on  $b$ ,  $c_0$  and  $c_1$  such that for all  $x$ ,*

$$\text{lfs}(x, C) \leq \text{lfs}(x, \hat{C}) \leq \frac{K}{\sin \alpha_1 \sin \alpha_2} \text{lfs}(x, C).$$

*Remark 5.* Recall that  $\bar{C}$  is the PSC containing the input and the collar construction. Lemma 8 is shown by first showing

$$\text{lfs}(x, \hat{C}) \leq \text{lfs}(x, \bar{C}) \leq K \text{lfs}(x, \hat{C}),$$

and then applying Lemma 5.

(REFINE) Protected Delaunay Refinement

In a similar fashion to the Delaunay refinement algorithm of Cheng and Poon [5], the PSC  $\hat{C}$  has been constructed without any acute angles in the non-intestine region so that Delaunay refinement can be performed. The analysis

of this approach involves an understanding of the Delaunay refinement of smooth surfaces in 3D. The intermediate PSC  $\tilde{C}$  including the collar region is much simpler from this perspective as all 2D faces in the complex are affine. While the collar approach involved elements of the analysis for 2D PSCs, the analysis of the intestine approach more closely resembles the much less complete theory of the refinement of 3D PSCs [5, 3, 15, 7].

We now consider two different approaches to performing a quality refinement of the non-intestine region. The first is to perform the usual Delaunay refinement and split smooth surfaces by projecting the circumcenter of any Delaunay triangle in the face to the surface. This is described in Algorithm 6. This approach suffers from one minor drawback: the Delaunay tetrahedralization inside the cylindrical regions of the intestine may not conform to the input. To eliminate this issue, the second approach is to impose more structure on the refinement of these cylindrical regions. This algorithm is given in Algorithm 7. Figure 4 shows the difference between the refinement around required cylindrical surfaces of the two algorithms.

**Algorithm 6** 3D Delaunay Refinement With Intestine - Unstructured

Action	Project the circumcenter of a simplex to its associated surface or curve and insert this vertex, unless it causes a lower-dimensional simplex to be unacceptable. In this case, queue the lower-dimensional object.
Priority	Simplices are prioritized by dimension, with lower-dimensional items processed first.
Unacceptability	A simplex in the non-intestine region is unacceptable if it has a nonempty circumball. A tetrahedron is unacceptable if its radius-edge ratio is larger than $\tau$ .
Safety	All simplices are safe to split.

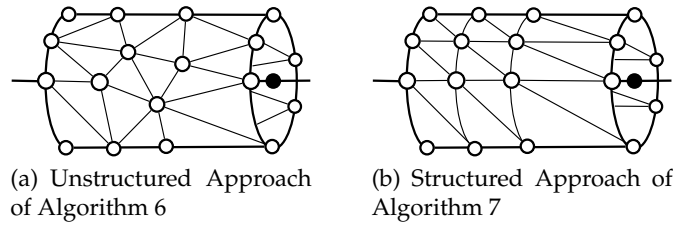


**Fig. 4.** Refinement of cylindrical surfaces around the intestine.

These algorithms terminate and produce meshes which are graded to the local feature size. This is summarized in the following theorem.

**Algorithm 7** 3D Delaunay Refinement With Intestine - Structured

Action	Project the circumcenter of a simplex to its associated surface or curve and insert this vertex, unless it causes a lower-dimensional simplex to be unacceptable. In this case, queue the lower-dimensional object. EXCEPTION: when handling a triangle associated with a cylindrical region which did not yield to another simplex, divide this cylindrical region into two cylinders of equal length and include the new boundary circle in the PSC. Moreover, insert vertices on this circle in the same fashion as in the construction of the intestine region.
Priority	Simplices are prioritized by dimension, with lower-dimensional items processed first.
Unacceptability	A simplex in the non-intestine region is unacceptable if it has a nonempty circumball. A tetrahedron is unacceptable if its radius-edge ratio is larger than $\tau$ .
Safety	All simplices are safe to split.

**Theorem 7.** *For any  $\tau > 4$ , there exists  $K > 0$  depending only upon  $\tau$ ,  $b$ ,  $c_0$ , and  $c_1$  such that for each vertex  $q$  inserted by Algorithm 6 or Algorithm 7,*

$$\text{lfs}(q, C) \leq \frac{K}{\sin \alpha_1 \sin \alpha_2} r_q.$$

*Remark 6.* The restriction  $\tau > 4$  is stronger than the restriction  $\tau > 2$  seen in Theorem 5. The techniques of Theorem 3 have not yet been extended to the case of curved surfaces, and without these techniques, the stronger condition on  $\tau$  is necessary. Extending this result to admit all  $\tau > 2$  is a topic of ongoing research.

Algorithm 7 produces a conforming Delaunay tetrahedralization of the input. This is shown in the next theorem.

**Theorem 8.** *Algorithm 7 produces a conforming Delaunay tetrahedralization of  $C$ . All tetrahedra with radius-edge ratio larger than  $\tau$  lie in the intestine region.*

The previous result does not hold for Algorithm 6, as the resulting mesh may not conform to the input. This may occur when a vertex on the boundary of the cylindrical region encroaches upon a triangle in a required face inside the intestine region.

However, a simple conforming (but not Delaunay) tetrahedralization of the intestine region does exist. The spheres around input vertices are tetrahedralized using the Delaunay tetrahedra. For the cylindrical sections, let  $p_1$  and  $p_2$  be the endpoints of the corresponding input segment. The tetrahedralization is produced with two types of tetrahedra.

- For any Delaunay triangle  $t$  on the boundary of the cylinder, include the tetrahedron with base  $t$  and vertex at  $p_1$ .

- For any arc  $s$  on the circle around  $p_2$ , include the tetrahedra with vertices  $p_1, p_2$  and the endpoints of  $s$ .

These tetrahedra are depicted in Figure 5. This construction yields a mesh which conforms to the input. This is summarized in the following theorem.

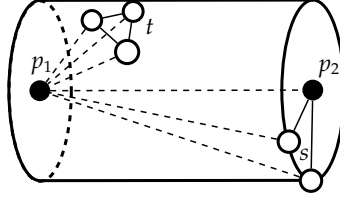


**Fig. 5.** Two types of tetrahedra are used to produce a conforming tetrahedralization of the intestine region following Algorithm 6.

**Theorem 9.** *Algorithm 6 produces a conforming Delaunay tetrahedralization of the non-intestine region of  $\hat{C}$ . The previous construction yields a conforming tetrahedralization of the intestine region of  $\hat{C}$  which matches the Delaunay tetrahedralization on the boundary of the intestine region. All tetrahedra with radius-edge ratio larger than  $\tau$  lie in the intestine region.*

## 5 Implementation Details and Examples

In 3D, we have implemented both collar and intestine based protection schemes. Our implementation relies on estimates of the local feature size given by a different Delaunay refinement algorithm [13, 14]. Algorithm 6 (rather than Algorithm 7) has been implemented and will be referred to as the intestine approach in the examples below. In the future, we hope to implement both algorithms and do a thorough comparison.

Figure 6 demonstrates both protection strategies on a very simple PLC: a single tetrahedra. Figure 7 shows the refinement of a single face of the pyramid during this refinement using the collar. The result looks very similar when using the intestine approach.

An essential method for reducing the number of vertices in the final mesh is to protect only input segments and vertices which are part of acute input angles. This yields a substantial improvement in the output mesh size. Figure 8 shows an input PLC, the resulting mesh when all segments are protected, and the resulting mesh when only acute input segments are protected. The resulting mesh with full protection contains 18079 vertices while the mesh with partial protection only contains 3216 vertices.

Finally, Figure 9 contains six examples produced by Algorithm 5. Data on the input and output sizes of the meshes produced for each of these examples

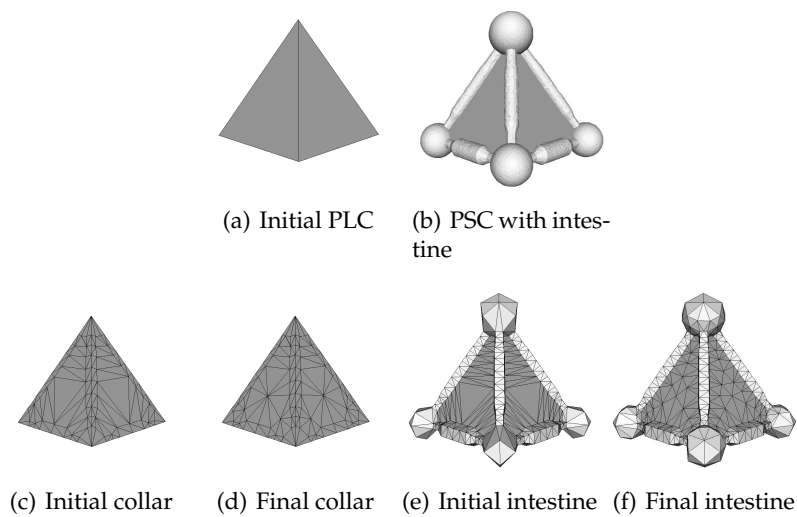


**Fig. 6.** Refinement of a simple pyramid.

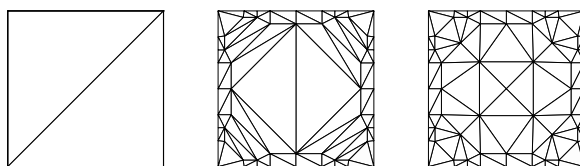


**Fig. 7.** Refinement of the base of the pyramid.

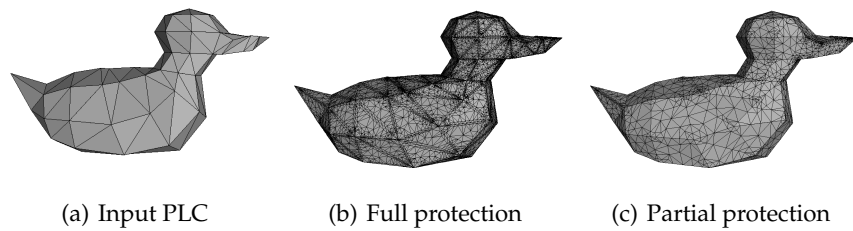


**Fig. 8.** Comparison of full and partial collar protection.



is contained in Table 1. Each of the meshes produced only uses the partial collar described above. While the refinement is performed in a bounding box, this bounding box was removed for the PLCs which enclose a volume. This is indicated in the “Box” column of Table 1.

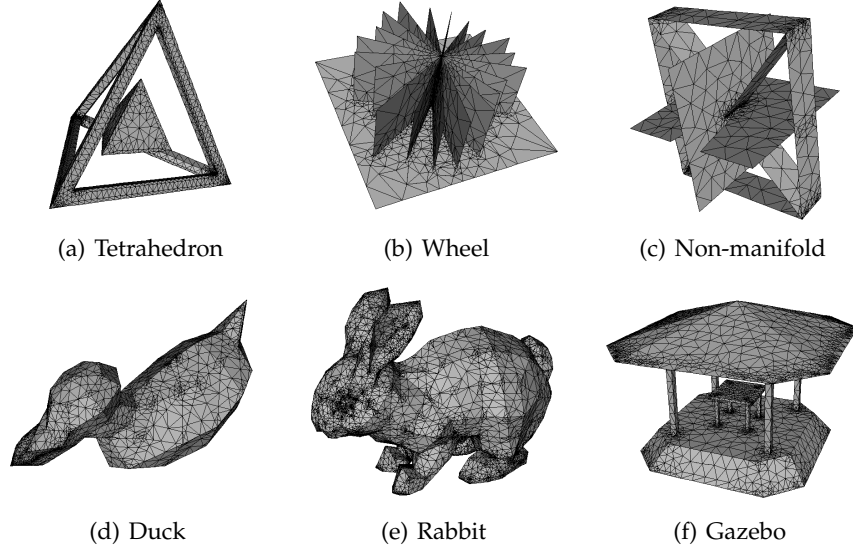


Fig. 9. Examples meshes produced by Algorithm 5.

Table 1. Results of Algorithm 5 on six PLCs with acute angles.

Name	Input			Output		
	Vertices	Segments	Faces	Vertices	Tetrahedra	Box
Tetrahedron	24	54	28	3700	11476	No
Wheel	46	65	21	4397	27182	Yes
Non-manifold	22	35	10	2498	15142	Yes
Duck	93	273	182	3216	11001	No
Rabbit	453	1353	902	18968	69001	No
Gazebo	97	148	57	4868	15318	No

## References

1. C. Boivin and C. Ollivier-Gooch. Guaranteed-quality triangular mesh generation for domains with curved boundaries. *International Journal for Numerical Methods*

- in Engineering*, 55(10):1185–1213, 2002.
2. D. E. Cardoze, G. L. Miller, M. Olah, and T. Phillips. A Bezier-based moving mesh framework for simulation with elastic membranes. In *Proceedings of the 13th International Meshing Roundtable*, pages 71–80, 2004.
3. S.-W. Cheng, T. K. Dey, and J. A. Levine. A practical Delaunay meshing algorithm for a large class of domains. In *Proceedings of the 16th International Meshing Roundtable*, pages 477–494, 2007.
4. S.-W. Cheng, T. K. Dey, and E. A. Ramos. Delaunay refinement for piecewise smooth complexes. In *Proceedings of the 18th Annual ACM-SIAM Symposium on Discrete Algorithms*, pages 1096–1105, 2007.
5. S.-W. Cheng and S.-H. Poon. Three-dimensional Delaunay mesh generation. In *Proceedings of the 14th Annual ACM-SIAM Symposium on Discrete Algorithms*, pages 295–304, 2003.
6. D. Cohen-Steiner, E. Colin de Verdière, and M. Yvinec. Conforming Delaunay triangulations in 3D. *Computational Geometry: Theory and Applications*, 28(2-3):217–233, 2004.
7. B. Hudson. Safe Steiner points for delaunay refinement. Research Notes of the 17th International Meshing Roundtable, 2008.
8. G. L. Miller, S. E. Pav, and N. J. Walkington. When and why Ruppert’s algorithm works. In *Proceedings of the 12th International Meshing Roundtable*, pages 91–102, 2003.
9. G. L. Miller, T. Phillips, and D. Sheehy. Fast sizing calculations for meshing. In *18th Fall Workshop on Computational Geometry*, 2008.
10. M. Murphy, D. M. Mount, and C. W. Gable. A point-placement strategy for conforming Delaunay tetrahedralization. *International Journal of Computational Geometry and Applications*, 11(6):669–682, 2001.
11. S. E. Pav and N. J. Walkington. Robust three dimensional Delaunay refinement. In *Proceedings of the 13th International Meshing Roundtable*, pages 145–156, 2004.
12. S. E. Pav and N. J. Walkington. Delaunay refinement by corner lopping. In *Proceedings of the 14th International Meshing Roundtable*, pages 165–181, 2005.
13. A. Rand and N. Walkington. 3D Delaunay refinement of sharp domains without a local feature size oracle. In *Proceedings of the 17th International Meshing Roundtable*, 2008.
14. A. Rand and N. Walkington. Delaunay refinement algorithms for estimating local feature size, 2009. Submitted.
15. L. Rineau and M. Yvinec. Meshing 3D domains bounded by piecewise smooth surfaces. In *Proceedings of the 16th International Meshing Roundtable*, pages 443–460, 2007.
16. J. Ruppert. A Delaunay refinement algorithm for quality 2-dimensional mesh generation. *Journal of Algorithms*, 18(3):548–585, 1995.
17. J. R. Shewchuk. Mesh generation for domains with small angles. In *Proceedings of the 16th Annual Symposium on Computational Geometry*, pages 1–10, 2000.
18. H. Si. On refinement of constrained Delaunay tetrahedralizations. In *Proceedings of the 15th International Meshing Roundtable*, pages 510–528, 2006.
19. H. Si and K. Gartner. Meshing piecewise linear complexes by constrained Delaunay tetrahedralizations. In *Proceedings of the 14th International Meshing Roundtable*, pages 147–163, 2005.